IEEE Access
Multidisciplinary | Rapid Review | Open Access Journal

Received 19 June 2023, accepted 2 August 2023, date of publication 8 August 2023, date of current version 16 August 2023.

Digital Object Identifier 10.1109/ACCESS.2023.3303089

RESEARCH ARTICLE

Parallel Blind Adaptive Equalization of Improved Block Constant Modulus Algorithm With Decision-Directed Mode

YING CHEN[1], GEQI WENG[2], SHENJI LUAN[1], YANHAI SHANG[1], CHAO LIU[1], AND JIANRONG BAO[3], (Senior Member, IEEE)

[1]Information Engineering School, Hangzhou Dianzi University, Hangzhou, Zhejiang 311305, China
[2]Department of Technology Development, Hangzhou Kylin Technology Company Ltd., Hangzhou, Zhejiang 310051, China
[3]School of Communication Engineering, Hangzhou Dianzi University, Hangzhou, Zhejiang 310018, China

Corresponding author: Shenji Luan (luanshenji@hdu.edu.cn)

This work was supported in part by the National Natural Science Foundation of China under Grant U1809201, in part by the Fundamental Research Funds for the Provincial Universities of Zhejiang under Grant GK209907299001-003, in part by the Zhejiang Provincial Natural Science Foundation of China under Grant LDT23F01014F01, and in part by the 2020 Domestic Visiting Scholars Program at Higher Education Institutions of China under Grant FX2020011.

ABSTRACT To eliminate inter-symbol interferences (ISI) caused by nonlinear group delay effect in high-speed broadband satellite sensor networks, an efficient parallel adaptive blind equalization of improved block constant modulus algorithm (IBCMA) with decision-directed (DD) mode (IBCMA-DD) is proposed with block minimum mean square error (MMSE) criterion. First, nonlinear group delay models are introduced in satellite channels. Second, the criterion of the classical Godard's constant modulus algorithm (CMA) is derived in the block vector form as the IBCMA for satellite signals with inter-symbol interference (ISI) caused by the above satellite channels. In the IBCMA, stochastic gradient descent and block minimum mean square error are adopted to reduce excess errors in equalization by adjusting block tap-weight vectors adaptively. Finally, the IBCMA is combined with the DD mode of equalization to both accelerate the parallel blind equalization with low complexity and improve the spectrum efficiency without any training data to occupy unnecessary bandwidth. Simulation results indicate that the proposed IBCMA-DD equalization possesses good performance in approaching ideal non-ISI transmissions. It achieves good bit error rate (BER) performance just within 0.3 dB of the theoretic performance under high signal-to-noise ratios (SNRs), even at satellite group delay channels by high-power nonlinear broadband filters. Therefore, it obtains excellent equalization under severely deteriorated group delay channels in broadband satellite sensor networks with high data rate.

INDEX TERMS Parallel equalization, blind adaptive equalization, improved block constant modulus algorithm, block minimum mean square error, intersymbol interference.

I. INTRODUCTION

High speed parallel blind adaptive equalization has been widely studied as one of the key technologies in wireless communications [1]. In practice, the non-idealization of both the channel and digital filter's truncation easily caused the ISI, limited bandwidth and nonlinear filter effect [1]. They resulted in a severe degrade in performance and thus seriously affected the communication quality. Traditional time domain equalizer was designed in the serial form and it received training sequences separately at the cost of low channel bandwidth utilization [2]. The ISI by the channel response was usually unpredictable and time varying [3], and then a blind and adaptive equalization was first proposed to compensate the ISI as in [4] and [5]. Subsequently, Godard proposed a blind equalization, *i.e.*, the classical CMA [6], and applied it to transmitted signals with constant envelope. It soon turned out to be a classic blind equalization with low

The associate editor coordinating the review of this manuscript and approving it for publication was Felix Albu.

computational complexity and easy implementation, and so on. However, the convergence speed rate was rather slow and the steady state error was still large [7]. Simultaneously, with the development of high speed satellite communications, the serial equalization was unable to fulfill the high speed transmissions. Therefore, efficient parallel blind equalization architecture for constant modulus signals was imperative in satellite communications.

Recently, with the rapid development of broadband satellite communications with high data rate, satellite modems easily encountered severe ISI caused by bandwidth constraint, group delay of nonlinear analogy filters, and so on [8]. To overcome these problems, equalizers, especially in the adaptive and blind form, were employed to eliminate them with adequate bandwidth efficiency. Then, two common Bussgang-like equalization, the CMA and DD mode [9], were used with low complexity in practice. In the former, the output of the CMA equalization approached the radius of statistics as constant modulus with robust convergence. But it was featured with poor performance of large mean square excess errors and phase rotation problems. Furthermore, there were still local convergence problems in the CMA due to the gradient based iterations in the adaptive equalization [10]. Then, the fractionally-spaced CMA blind equalizer cost function was analyzed for the local minima [11] and misconvergence was observed in the constant modulus adaptive algorithm [12]. On acoustic digital links adopting pulse position modulation in severe multipath shallow water scenarios, the blind fractionally spaced channel equalization can be performed with high feasibility by using fractional sampling and a suitably modified Bussgang scheme of memory non-linearity at the receiver side [13]. In addition, it was further improved for global convergence by using CMA robustness and related new processing techniques to combat channel noises and lack of disparity [14], [15], [16]. The tracking issues of this blind equalization was also analyzed for the CMA robustness [7]. In the latter, the output of DD equalization approached the constellation points and corrected the phase rotation for extremely small excess errors. However, it was hard for the DD mode to open the eye pattern at low SNRS and the use of misjudgment metrics of the hard decision of modulated samples caused the error propagation phenomenon to deteriorate the performance. In conclusion, they can be combined together as dual-mode equalization to both exploit their advantages and avoid their weakness. In addition, the efficient combination of the soft switch and dual-mode of both the CMA and DD mode in equalization had become research hot spots. For variable modulation, a simple and robust variable modulation-decision-directed least mean square (VM-DDLMS) algorithm was proposed to reduce the complexity of conventional equalization and improve the stability of variable modulation (VM) systems [17]. It was implemented in the form of serial mode at the cost of much larger equalization latency and slower error convergence. Subsequently, limited by hardware speed, parallel architecture for fast digital signal processing was widely adopted in the implementation of modern digital systems with high data rates. Specifically, parallel adaptive equalization can be employed to eliminate ISIs much efficiently. For non-blind parallel equalization, a new adaptive parallel equalization structure, called block least minimum square (BLMS), was suggested in the block implementation of the serial least minimum square (LMS) [18]. However, the training-sequences-based block parallel equalization performed with more spectrum efficiency loss due to the sequences occupying quite a lot of bandwidth. A semi-blind equalization was proposed to improve performance of both the mean-squared error and bit error rate for simultaneously cancelling the self-interference component and estimating the propagation channel in the fifth-generation (5G) quasi-cyclic low-density parity-check encoded short-packet full-duplex transmissions [19]. But it still requires a small number of pilot symbols to be transmitted accurately for reference signals in equalization and it was difficult in severely distorted channels. Moreover, it was impracticable in a multipoint network due to different channel link states among these network nodes [6]. Other than the Bussgang-like scheme, the high-order moment and cyclostationarity of source signals were employed in In airborne passive bistatic radar to construct the new cost function for the phase constraint and solve the problem for the better convergence with a complex value back propagation neural network [20]. But the complexity and processing latency were the hinder for practical application. In addition, Turbo blind equalization was also proposed by establishing a new expectation-maximization Viterbi algorithm and turbo scheme [21]. The convergence, bit error rate, and real-time performance were achieved effectively by the improved exchange of extrinsic information and stopping criterion. But it still required well initial equalization circumstance of success Viterbi decoding. Except for the aforementioned deficiencies of the CMA, it also suffered from the problems of the phase rotation, large remain error, and slow convergence caused by the nature of the CMA, which hindered it to be efficiently implemented in practice.

According to the current status of equalization in literature, we mainly propose a new implementation of block parallel CMA equalization scheme, *i.e.*, the IBCMA-DD, to accomplish efficient equalization. Our scheme mainly takes full use of Godard's constant modulus and block minimum mean-square error (MMSE) to derive a new optimized blind equalization. Then, the corresponding theoretical derivation and numerical simulations are performed to verify the effectiveness of our method. In this scheme, the block processing with steep stair descendent of the BLMS [22] is extended to the proposed IBCMA. Then, the block MMSE-based performance criterion is defined and derived with a gradient estimate of a correction between the desired and input signals. It adjusts the tap-weight vector to both satisfy the criterion and obtain convergence. The large mean square excess errors [23] and phase rotation problems are then compensated by the successive DD mode for better performance. Besides,

the blind deconvolution [24], [25] are also analyzed for the proposed IBCMA equalization with good performance. In addition, the architecture of the proposed scheme is also given for practical equalization. In practice, the fractional CMA with DD mode is adopted to overcome both the phase rotation and large remainder errors with the help of the known sequence of frame synchronization head. Accordingly, the proposed block implementation of parallel CMA equalization is employed to speed up the equalization and thus eliminate the slow convergence problem for fast equalization and less latency. Finally, the main contributions are concluded as follows.

- **Construction of nonlinear group delay models for the satellite channels.**
  Nonlinear group delay models are constructed and introduced to simulate satellite channels. Given expected amplitude-frequency response of the channel and the magnitude response of the group delay, the weighted square error cost function about the amplitude-frequency and response of the group delay is constructed for the estimation of the equalization.
- **Derivation of the block MMSE-based performance criterion for the IBCMA with a gradient estimate of a correction between the desired and input signals.**
  The criterion of the classical CMA is derived in the block vector form as the IBCMA for satellite signals with inter-symbol interference (ISI) caused by the above satellite channels. In the IBCMA, stochastic gradient descent and block minimum mean square error are adopted to reduce excess errors in equalization by adjusting block tap-weight vectors adaptively.
- **Practical IBCMA-DD scheme to accelerate the parallel blind equalization, improve the spectrum efficiency and compensate the residual mean square excess errors and phase rotation.**
  The IBCMA is combined with the DD mode to both accelerate the parallel blind equalization with low complexity and improve the spectrum efficiency without any training data to occupy unnecessary bandwidth. In addition, the large mean square excess errors and phase rotation problems are then compensated by the successive DD mode for better performance.

This paper is organized as follows. In Section II, nonlinear group delay channel model is introduced for satellite channels. Section III mainly presents the derivation of the parallel block MMSE-based blind equalization, *i.e.*, the IBCMA-DD. Also the detailed presentation of the proposed IBCMA-DD is given with theoretic analyses to elaborate the whole procedure. Subsequently, numerical simulations and corresponding analyses of the proposed parallel blind adaptive IBCMA-DD equalization, conducted in the presence of noises and severe nonlinear group delay channels, are given to manifest the good convergence in Section IV. Finally, the conclusion is drawn in Section V.

II. PRINCIPLE OF EQUALIZATION AND NONLINEAR GROUP DELAY MODEL

A. PRINCIPLE OF EQUALIZATION

Equalization is actually the deconvolution of the channel impulse response and the cascade of them can be modeled as the convolution of them according to the principle of signals and systems [26]. An equivalent base band model of a typical equalizer [27] is illustrated in Fig. 1. To provide maximum power in the satellite downlink, a high power amplifier (HPA), *e.g.*, traveling wave tube amplifier (TWTA), is operated close to saturation, which easily causes the nonlinear group delay ISI channel. And it can be modeled as a channel filter with group delay distortion similar to that of a digital beam forming system [28].

In Fig. 1, $\{s(n)\}$ is the original signals to be sent in the source. $\{h(n)\}$ is the unknown channel impulse response with length N_h. $\{v(n)\}$ is additive white Gaussian noises. The equalizer acquires information from the received signals $\{r(n)\}$ and then it performs the equalization and thus adaptively adjusts the weighted or tap coefficients $\{f(n)\}$ of the equalizer with length N_h. Subsequently, the output $y(n)$ of the equalizer is the optimal estimation of $s(n)$. Given small discrepancy between $y(n)$ and $s(n)$, the output of $\hat{s}(n)$ by final decision is the recovered data $s(n)$.

B. NONLINEAR GROUP DELAY CHANNEL MODEL

Group signals are complex signals or wave group by several frequency band and in some special form. When the group signals pass through a communication system, the latency caused by the entire waveform of the group signals is defined as the group delay effect [28]. It is used to distinguish different frequency component of the group signals. Therefore, the concept and properties of the group delay are concluded as follows.

Suppose that the characteristic function of the frequency response in communication channels is represented as

$$H(e^{j\omega}) = \left|H(e^{j\omega})\right| e^{j\varphi(\omega)}, \tag{1}$$

where $\left|H(e^{j\omega})\right|$ and $\varphi(\omega)$ are the characteristic function of the amplitude- and phase-frequency, respectively. The function of the group delay $\tau(\omega)$ is then defined as

$$\tau(\omega) = -d\varphi(\omega)/d\omega. \tag{2}$$

The characteristic function of the group delay is actually the 1-order differential or derivative of the phase-frequency characteristic function $\varphi(\omega)$ to the angle frequency ω with a negative symbol. If $\tau(\omega)$ is a constant, there is a linear relationship between $\varphi(\omega)$ and ω. Then, different frequency components of signals have the same group delay, and no distortion occurs in the transmitted signals. Otherwise, there are nonlinear group delay distortions for the signals and the performance of received signals are degrade. Finally, the group delay model is represented as follows.

The channel impulse response is presented as $h = [h(0), h(1), \cdots, h(N-1)]^T$, where N is the length of the

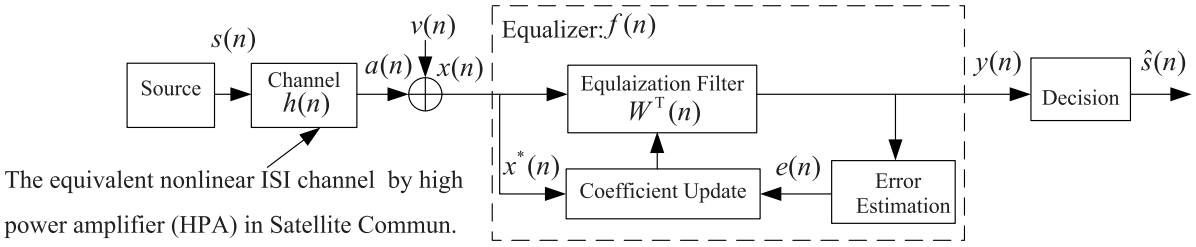

FIGURE 1. Equivalent baseband model of a typical adaptive equalizer to combat the nonlinear ISI channel, especially in stellite communications.

channel filter. Then, the frequency response function of the channel is expressed as

$$H(e^{j\omega}) = \sum_{n=0}^{N-1} h(n)e^{-jn\omega} = \left|H(e^{j\omega})\right| e^{j\phi(\omega)}. \tag{3}$$

Subsequently, the frequency response function of the group delay is given as

$$\tau(\omega) = -\frac{d\varphi(\omega)}{d\omega} = Re\left\{\frac{\sum_{n=0}^{N-1} nh(n)e^{-jn\omega}}{\sum_{n=0}^{N-1} h(n)e^{-jn\omega}}\right\}, \tag{4}$$

where "$Re[\cdot]$" represents the function to acquire the real part of a complex.

Given expected amplitude-frequency response of the channel $\left|H_d(e^{j\omega})\right|$ and the magnitude response of the group delay $\tau_d(\omega)$, the weighted square error cost function about the amplitude-frequency and response of the group delay is constructed. Subsequently, it participates the equalization computation and coefficient update in the complex mode of the equalization. Therefore, the error cost function of the group delay model is derived as

$$\begin{aligned} e = \alpha \cdot \int_{\omega\in P,S} \left[\left|H(e^{j\omega})\right| - \left|H_d(e^{j\omega})\right|\right]^2 d\omega \\ + \int_{\omega\in P} |\tau(\omega) - \tau_d(\omega)|^2 d\omega, \end{aligned} \tag{5}$$

where P and S represent the pass and stop bands, and α is the amplitude weight in the cost function, respectively.

By the discrete of the frequency, the above error cost function of the group delay is deduced as

$$\begin{aligned} e = \alpha \cdot \sum_{\omega_i\in P,S} \left[\left|H(e^{j\omega_i})\right| - \left|H_d(e^{j\omega_i})\right|\right]^2 \\ + \sum_{\omega_i\in P} |\tau(\omega_i) - \tau_d(\omega_i)|^2, \end{aligned} \tag{6}$$

where "ω_i" is the same as ω in the discrete form as the i-th ω.

Finally, the finite impulse response of the group delay can be designed as an optimization objective function and it is represented as

$$\min_h e = \alpha \cdot \sum_{\omega_i\in P,S} |e_H(\omega_i)|^2 + \sum_{\omega_i\in P} |e_\tau(\omega_i)|^2. \tag{7}$$

This optimization function is actually equivalent to the solution of the channel coefficients h to minimize the cost function of the weighted square errors. Finally, the results of the group delay filter can be accomplished by efficient solution of (7).

III. EFFICIENT MMSE-BASED IBCMA WITH DD MODE FOR PARALLEL BLIND ADAPTIVE EQUALIZATION

In this section, the process of the MMSE-based IBCMA is proposed and derived at first and then the whole procedure of the efficient MMSE-DDM is generated for parallel blind adaptive equalization. The equalization can be performed in two stage, *i.e.*, the first capturing stage and the second tracking one. Corresponding, it firstly uses the proposed IBCMA to acquire the raw equalization in the first capturing stage to open the eye in the eye pattern of the modulated signals. Subsequently, it adopts the block LMS algorithm [18] with hard decision as reference values to obtain the fine equalization in the second tracking stage for better equalization performance.

The entire flow of the proposed scheme is listed as follows. First, a brief retrospect of the CMA procedure is given. Second, IBCMA is derived with the MMSE criterion of the CMA. Third, the DD mode is adopted with the Block LMS algorithm after the raw equalization by the proposed IBCMA. Finally, the whole diagram of the efficient MMSE-based IBCMA-DD is suggested for practical use. They are described respectively as follows.

A. BRIEF RETROSPECT OF THE CLASSIC CMA SCHEME

Due to long distance in satellite communications, power efficient low order modulation, such as the quadrature phase shift keying (QPSK), is widely used in satellite communications efficiently. Then, the channel output of a QPSK modulation system is described by using the baseband representation as

$$x(t) = \sum_n a_n h(t - nT - t_0) + v(t), \tag{8}$$

where a sequence of independent identically distributed (*i.i.d*) complex data $\{a_n\}$ are sent by the transmitter over a channel with the baseband equivalent impulse response $h(t)$. $v(t)$ is the complex additive white Gaussian noise (AWGN) of zero-mean stationary complex Gaussian noise with modest

variance and it is independent of the input a_n. t_0 is the delay of the sample time. The aim of the equalization is to find a transfer function $w(t)$ to compensate ISI brought by satellite channels. Although we mainly consider a tapped delay-line equalizer of a tap space equal to T, the analysis is also extended to fractionally spaced equalizers [11], [14], [15].

In T–spaced equalizer (TSE) systems, the channel output is sampled at the baud rate $1/T$ and it is expressed as

$$x(nt) = \sum_{k=0}^{\infty} a_k h(nT - kT - t_0) + v(nT). \tag{9}$$

To simplify the analyses, we define some notations as

$$x_n = x(nt),\ h_n = h(nT - t_0),\ v_n = v(nT). \tag{10}$$

Subsequently, (9) is rewritten as the form of discrete convolution with noises as

$$x_n = \sum_{k=0}^{\infty} a_k h_{n-k} + v_n = a_k \otimes h_n + v_n. \tag{11}$$

The TSE is then designed as a finite impulse response (FIR) filter with coefficient vector $[w_1, \cdots, w_N]^T$ to remove the ISI from the equalizer as

$$y_n = \sum_{k=1}^{N} w_k x_{n-k}. \tag{12}$$

From Godard's constant modulus principle [6], the CMA ($p = 2$) aims to minimize the cost function of the constant modulus as

$$J_2 = \frac{1}{4} E\{(|y_n|^2 - R_2)^2\},\ with\ R_2 = \frac{E(|a_n|^4)}{E(|a_n|^2)}. \tag{13}$$

According to this criterion, the widely used CMA [6] is written for general procedures as

$$X_k = [x_k, x_{k-1}, \cdots, x_{k-L+1}]^T, \tag{14}$$
$$W_k = [w_1, w_2, \cdots, w_L]^T, \tag{15}$$
$$y_k = X_k^T \cdot W_k^*, \tag{16}$$
$$e_k = y_k \cdot (R_2 - |y_k|^2), \tag{17}$$
$$W_{k+1} = W_k + \mu \cdot X_k \cdot e_k^*, \tag{18}$$

where x_k and y_k are, respectively, the original input signals needed to be equalized and the output signals after equalization, X_k and W_k are, respectively, the $L \times 1$ input signal vector and tap-weight vector (W_k is actually the conjugative value of c_k in (28) of Godard's paper [6]), μ is the step-size parameter, R_2 is the constant modulus of input signal ($R_p, p = 2$) and e_k is the error to adjust the tap-weight vector. In addition, W_k is initially assigned with the value as $[1, 0, \cdots, 0]$ and $x_k = 0, k \leq 0$ for initialization.

B. PROPOSED IBCMA SCHEME WITH DERIVATION AND ANALYSES

As the preface of this section, the equalization can be performed in two stage, *i.e.*, the capturing IBCMA and tracking DD stages. They are performed in sequence as follows.

In the proposed IBCMA, the serial input signals are firstly organized in the form of block matrix. In the matrix, L is set as the block length and the numbers of vector in a block to simplify the computation. k is the block sequence number in the proposed scheme, *e.g.*, the k-th block CMA equalization procedure. Subsequently, the initial and typical blocks are listed as

$$\chi_k = [X_{(k-1)L+1}, \cdots, X_{kL}]^T = \begin{pmatrix} x_{(k-1)L+1} & \cdots & x_{kL} \\ \vdots & \ddots & \vdots \\ x_{kL} & \cdots & x_{(k+1)L-1} \end{pmatrix} \tag{19}$$

Similar to the block LMS algorithm [18], an MMSE based block CMA is derived to sequentially solve the tap-weight vector by a gradient adjust technique. Because the tap-weight is desired to keep constant under each block data processing, the tap-weight vector is adjusted once per data block to achieve the parallel effect. The core of the proposed algorithm is then to restrain the square of error to minimum and thus it is consistent with the block MMSE criterion. Hence, the improved block equalization is derived and listed as

$$Y_k = \chi_k \cdot W_k^*, \tag{20}$$
$$W_{k+1} = W_k - \mu_{IBCMA} \cdot \nabla_{Bk}, \tag{21}$$

where Y_k is the output vector of length L as $[y_{(k-1)L+1}, y_{(k-1)L+2}, \cdots, y_{kL}]^T$ and it is denoted as $[y_1^{(k)}, y_2^{(k)}, \cdots, y_L^{(k)}]^T$. μ_{IBCMA} is the step-size parameter, ∇_{Bk} and W_k are the $L \times 1$ block MMSE gradient and tap-weight vector at the k-th block, respectively, where W_k is assigned with the same initial value as the above serial CMA.

By the block LMS criterion, the gradient is taken with respect to the estimated error and the tap-weight vector and it is expressed as

$$\nabla_{Bk} = C \cdot \left. \frac{\partial E[\varepsilon_k^T \varepsilon_k^*]}{\partial W} \right|_{W=W_k}, \tag{22}$$

where C is a constant related to fixed parameter L and it can be incorporated into the step-size parameter μ_{IBCMA} in the equalization calculation. ε_k is the $L \times 1$ error vector derived from (17) for the k-th block and it is represented as

$$\varepsilon_k = \begin{pmatrix} e_1^{(k)} \\ e_2^{(k)} \\ \vdots \\ e_L^{(k)} \end{pmatrix} = \begin{pmatrix} y_1^{(k)}(R_2 - \left|y_1^{(k)}\right|^2) \\ y_2^{(k)}(R_2 - \left|y_2^{(k)}\right|^2) \\ \vdots \\ y_L^{(k)}(R_2 - \left|y_L^{(k)}\right|^2) \end{pmatrix}. \tag{23}$$

Since the direct computation of the expectation of $\varepsilon_k^T \varepsilon_k^*$ is difficult, an estimate of the gradient, *i.e.*, $\hat{\nabla}_{Bk}$, is used in place of ∇_{Bk}. The MMSE-based gradient estimate, *i.e.*, $\hat{\nabla}_{Bk}$, at the k-th block replaces ∇_{Bk} in (21) and it is represented as

$$\hat{\nabla}_{Bk} = C \cdot \left.\frac{\partial[\varepsilon_k^T \varepsilon_k^*]}{\partial W}\right|_{W=W_k} = C \cdot \left.\frac{\partial \sum_{i=1}^{L} \left|e_i^{(k)}\right|^2}{\partial W}\right|_{W=W_k}. \quad (24)$$

To simplify the result of $\hat{\nabla}_{Bk}$, a variable $\alpha_{i,j}^{(k)}$ is defined to stand for the element in matrix χ_k with the coordinate (i, j) and it is easily mapped into the real element χ_k. By matrix analysis and the above relationship among the variables, $\hat{\nabla}_{Bk}$ can be further figured out as

$$\hat{\nabla}_{Bk} = 2C \cdot \begin{pmatrix} \sum_{i=1}^{L} \alpha_{i,1}^{(k)} \cdot (R_2 - 2 \cdot \left|y_i^{(k)}\right|^2) \cdot (e_i^{(k)})^* \\ \sum_{i=1}^{L} \alpha_{i,2}^{(k)} \cdot (R_2 - 2 \cdot \left|y_i^{(k)}\right|^2) \cdot (e_i^{(k)})^* \\ \vdots \\ \sum_{i=1}^{L} \alpha_{i,L}^{(k)} \cdot (R_2 - 2 \cdot \left|y_i^{(k)}\right|^2) \cdot (e_i^{(k)})^* \end{pmatrix}. \quad (25)$$

The detailed deduction of (25) is then presented as follows.

First, the received signals are organized as a data block χ_k with the i-th vector element of $X_{(k-1)L+i} = [x_{(k-1)L+i}, x_{(k-1)L+2}, \cdots, x_{(k-1)L+i}]^T$. For the convenient of successive derivation, the elements of matrix χ_k are all represented with element $\alpha_{i,j}^{(k)}$, which easily identify the coordination and iterative number (*e.g.*, k) of them. In other words, in the k-th iteration, there is $\alpha_{i,j}^{(k)} = x_{(k-1)L+i+j-1}$. Then, the data block χ_k is presented as

$$\chi_k = [X_{(k-1)L+1}, \cdots, X_{kL}]^T = \begin{pmatrix} \alpha_{1,1}^{(k)} & \cdots & \alpha_{1,L}^{(k)} \\ \vdots & \ddots & \vdots \\ \alpha_{L,1}^{(k)} & \cdots & \alpha_{L,L}^{(k)} \end{pmatrix}. \quad (26)$$

By the property of the derivative of the matrix, there are the following conclusions as

$$J(w) = A(w)B(w), \quad (27)$$

$$\frac{\partial J(w)}{\partial w} = \frac{\partial A(w)B(w)}{\partial w} = \frac{\partial A(w)}{\partial w} B(w) + \frac{\partial B(w)^H}{\partial w} A(w)^H \quad (28)$$

where $J(w)$, $A(w)$, and $B(w)$ are matrices with dependent variable vector w.

Therefore, if F is the row vector as $F = [F_1, \cdots, F_m]$, the derivative of it to column vector $W = [w_1, w_2, \cdots, w_L]^T$ is expressed as

$$\frac{\partial F}{\partial W} = \begin{pmatrix} \frac{\partial f_1}{\partial w_1} & \cdots & \frac{\partial f_m}{\partial w_1} \\ \vdots & \ddots & \vdots \\ \frac{\partial f_1}{\partial w_L} & \cdots & \frac{\partial f_m}{\partial w_L} \end{pmatrix}. \quad (29)$$

According to equations (27)-(29), (24) is deduced as

$$\begin{aligned} \hat{\nabla}_{Bk} &= C \cdot \left.\frac{\partial[\varepsilon_k^T \varepsilon_k^*]}{\partial W}\right|_{W=W_k} \\ &= C \cdot \{\frac{\partial[\varepsilon_k^T]}{\partial W_k} \cdot \varepsilon_k^* + \frac{\partial[\varepsilon_k^T]}{\partial W_k} \cdot \varepsilon_k^*\} \\ &= 2C \cdot \frac{\partial[\varepsilon_k^T]}{\partial W_k} \cdot \varepsilon_k^*. \end{aligned} \quad (30)$$

According to (29) and it is substituted by (23), (30) can be further derived as (31), as shown at the bottom of the next page.

Suppose that w_i is independent of w_j on the condition of $i \neq j$. Then, by substituting (26) into (31), also using (29) and the property of the partial derivative as $\frac{\partial F(w_j)}{\partial w_i} = 0, (i \neq j)$, there is the result for the iterative update of the gradient vector $\hat{\nabla}_{Bk}$ as (32), as shown at the bottom of the next page.

Subsequently, according to (26), there are (33), as shown at the bottom of the next page.

By (34), we obtain (35), as shown at the bottom of the next page.

Subsequently, (32) can be derived as (36), as shown at the bottom of page 8.

Therefore, (36) is deduced and organized for the final result of $\hat{\nabla}_{Bk}$ and it is exactly the same to (25). The temporally output $y(k)$ in the first capturing stage is then calculated by (20) and (21) until to the next stage.

In the second tracking stage of the DD equalization mode, the classic LMS algorithm is adopted with the hard decision of received signals as the expected response for the same signals. In addition, the LMS is parallel implemented in the form of the block LMS [18] and it is employed in our scheme of the DD mode. Therefore, the DD equalization mode is designed to be the successive procedure in the above IBCMA algorithm. Also a switch of the above two stages is established when the steady-state mean square error (MSE) of the IBCMA is less than the switch threshold. Simultaneously, the switch threshold can be obtained by the numerical calculation in numerical simulations, where the adjacent MSE of the IBCMA iteration approaches nearly together. Therefore, the switch can be made under very close MSE between adjacent iterations. Subsequently, the fine DD equalization is performed after the raw IBCMA equalization and the final equalization is accomplished.

The analysis of the IBCMA is just on the assumption of noiseless environment. Actually, the stable equalization is easily perturbed by the AWGNs in practice. But the position of the equalization remains in the neighborhood of the ideal equalization under noiseless channel when a modest amount of white channel noises are present. This fine property is mainly caused by the feature of adaptive algorithm and it can be illustrated by the numeric analysis in Section IV. Moreover, just as the analyses in [14], further better convergence of the proposed equalization is obtained by eliminating local convergence, when the fractionally-spaced equalizer (FSE) is adopted instead of the TSE.

C. PARALLEL BLIND ADAPTIVE EQUALIZATION STRUCTURE OF THE IBCMA WITH THE DD MODE

In this subsection, an implementation of the Parallel blind adaptive equalization of the IBCMA-DD is proposed. First, we present the entire flowchart of the proposed scheme for the IBCMA-DD. Then, the structure of the whole scheme is given for practical equalization. Finally, they are described as follows.

$$\hat{\nabla}_{Bk} = 2C \cdot \frac{\partial[\varepsilon_k^T]}{\partial W_k} \cdot \varepsilon_k^* = 2C \cdot \frac{\partial[\begin{pmatrix} y_1^{(k)}(R_2 - \left|y_1^{(k)}\right|^2) \\ y_2^{(k)}(R_2 - \left|y_2^{(k)}\right|^2) \\ \vdots \\ y_L^{(k)}(R_2 - \left|y_L^{(k)}\right|^2) \end{pmatrix}^T]}{\partial W_k} \cdot \begin{pmatrix} y_1^{(k)}(R_2 - \left|y_1^{(k)}\right|^2) \\ y_2^{(k)}(R_2 - \left|y_2^{(k)}\right|^2) \\ \vdots \\ y_L^{(k)}(R_2 - \left|y_L^{(k)}\right|^2) \end{pmatrix}^* . \tag{31}$$

$$\begin{aligned} \hat{\nabla}_{Bk} &= 2C \cdot \begin{pmatrix} \frac{\partial y_1^{(k)}(R_2 - \left|y_1^{(k)}\right|^2)}{\partial w_1} & \cdots & \frac{\partial y_L^{(k)}(R_2 - \left|y_L^{(k)}\right|^2)}{\partial w_1} \\ \vdots & \ddots & \vdots \\ \frac{\partial y_1^{(k)}(R_2 - \left|y_1^{(k)}\right|^2)}{\partial w_L} & \cdots & \frac{\partial y_L^{(k)}(R_2 - \left|y_L^{(k)}\right|^2)}{\partial w_L} \end{pmatrix} \cdot \begin{pmatrix} y_1^{(k)}(R_2 - \left|y_1^{(k)}\right|^2) \\ y_2^{(k)}(R_2 - \left|y_2^{(k)}\right|^2) \\ \vdots \\ y_L^{(k)}(R_2 - \left|y_L^{(k)}\right|^2) \end{pmatrix}^* \\ &= 2C \cdot \begin{pmatrix} \frac{\partial y_1^{(k)} R_2 - (y_1^{(k)})^2 \cdot (y_1^{(k)})^*)}{\partial w_1} & \cdots & \frac{\partial y_L^{(k)} R_2 - (y_L^{(k)})^2 \cdot (y_L^{(k)})^*)}{\partial w_1} \\ \vdots & \ddots & \vdots \\ \frac{\partial y_1^{(k)} R_2 - (y_1^{(k)})^2 \cdot (y_1^{(k)})^*)}{\partial w_L} & \cdots & \frac{\partial y_L^{(k)} R_2 - (y_L^{(k)})^2 \cdot (y_L^{(k)})^*)}{\partial w_L} \end{pmatrix} \cdot \begin{pmatrix} y_1^{(k)}(R_2 - \left|y_1^{(k)}\right|^2) \\ y_2^{(k)}(R_2 - \left|y_2^{(k)}\right|^2) \\ \vdots \\ y_L^{(k)}(R_2 - \left|y_L^{(k)}\right|^2) \end{pmatrix}^* \\ &= 2C \cdot \begin{pmatrix} \frac{\partial y_1^{(k)}}{\partial w_1}(R_2 - 2\left|y_1^{(k)}\right|^2) & \cdots & \frac{\partial y_L^{(k)}}{\partial w_1}(R_2 - 2\left|y_L^{(k)}\right|^2) \\ \vdots & \ddots & \vdots \\ \frac{\partial y_1^{(k)}}{\partial w_L}(R_2 - 2\left|y_1^{(k)}\right|^2) & \cdots & \frac{\partial y_L^{(k)}}{\partial w_L}(R_2 - 2\left|y_L^{(k)}\right|^2) \end{pmatrix} \cdot \begin{pmatrix} y_1^{(k)}(R_2 - \left|y_1^{(k)}\right|^2) \\ y_2^{(k)}(R_2 - \left|y_2^{(k)}\right|^2) \\ \vdots \\ y_L^{(k)}(R_2 - \left|y_L^{(k)}\right|^2) \end{pmatrix}^* . \end{aligned} \tag{32}$$

$$\chi_k = [X_{(k-1)L+1}, \cdots, X_{kL}]^T = \begin{pmatrix} \alpha_{1,1}^{(k)} & \cdots & \alpha_{1,L}^{(k)} \\ \vdots & \ddots & \vdots \\ \alpha_{L,1}^{(k)} & \cdots & \alpha_{L,L}^{(k)} \end{pmatrix} [w_1, w_2, \cdots, w_L]^T, \tag{33}$$

$$Y_k = [y_1^{(k)}, \cdots, y_L^{(k)}] = [\sum_{i=1}^{L} \alpha_{1,i}^{(k)} \cdot w_i, \cdots, \sum_{i=1}^{L} \alpha_{L,i}^{(k)} \cdot w_i]. \tag{34}$$

$$\frac{\partial y_1^{(k)}}{\partial w_1} = \frac{\sum_{i=1}^{L} \alpha_{1,i}^{(k)} \cdot w_i}{\partial w_1} = \alpha_{1,1}^{(k)}. \tag{35}$$

1) FLOW OF THE ENTIRE BLIND ADAPTIVE IBCMA-DD EQUALIZATION SCHEME

The entire blind adaptive equalization scheme is performed with two stages as the capturing and tracking stage, respectively. They are switched by a switch threshold decision. The detailed procedures of the proposed scheme is summarized and presented in Table 1.

With the same stable MSE as the equalization stop indicator, the DD mode is applied for much finer equalization. In the block LMS equalization for the parallel DD mode, the expected response of received signals are known signals to be sent to the destination by occupying some transmission bandwidth. However, the reference signals required in the LMS algorithm is not transmitted in channels. It uses the hard decision of received signals as the reference signals. For instance, the reference signals for a QPSK modulated signals are exactly one of the four constellation points, in which quadrant the modulated signals are located and the final hard decision is made.

2) IMPLEMENTATION OF THE ENTIRE BLIND ADAPTIVE EQUALIZATION SCHEME

Since the unblinded block LMS algorithm for the DD mode has been totally analyzed in [18], we mainly describe the implementation of the IBCMA. The structure of the DD mode can be incorporated into the IBCMA. According to the main procedures of the proposed parallel adaptive IBCMA equalization in the above subsection, it can be implemented with a parallel structure shown in Fig. 2.

In Fig. 2, the more complex module of the calculation of the stochastic gradient for the equalization iteration can be further decomposed and implemented in Fig. 3. All L-output elements of the stochastic gradient in Fig. 3 is combined together to generate the entire vector $\tilde{\nabla}_{Bk}$.

Finally, the proposed IBCMA is combined with the DD mode and the latter can be easily incorporated in to the module of the update of the tap coefficient. The error calculation in the iteration is just the subtraction between a signal and the hard decision of it, respectively. The complexity of the proposed scheme is large, since there is quite a lot of multiplication in the proposed scheme. However, in the parallel filtering of the proposed scheme, they can be improved with the frequency domain convolution calculation by faster Fourier transformation (FFT) efficiently.

IV. NUMERICAL SIMULATIONS AND RESULT ANALYSES

The effectiveness of the proposed IBCMA-DD is verified with numerical simulations in nonlinear satellite group delay channels. First, the typical group delay channels are numerically modeled according to the practical measured group delay distortion data from the traveling-wave tube amplifier (TWTA) of the Ka broadband satellite transponder [29]. Second, the above parallel blind adaptive IBCMA-DD equalization is simulated and analyzed to validate the good equalization effect. Finally, they are described as follows.

A. GROUP DELAY CHANNEL MODEL OF THE TWTA IN THE SATELLITE TRANSPONDER

The group delay channel model of the TWTA is modeled and designed as the infinite impulse response filter in the satellite transponder. The pass band bandwidth of the filter is configured as 200Mhz. The rated group delay difference in the pass band edge and the central frequency is set less than 10 nanosecond. The transmission rate is 100 Mbits/second. Therefore, the group delay is less than 10 symbol gaps in the range of the pass band. By [29], two typical category group delay channels are designed as follows.

- **Channel I**
  The main parameter for the base band group delay finite impulse response (FIR) channel is configured as follows. The number of the tap is 35. The normalized frequency of the pass band side is the 0.5. The normalized frequency of the stop band side is the 0.5. The group delay difference in the pass band edge and the central frequency is less than 5 symbol gaps. The weighted factor for the square difference of the amplitude is 100. The discrete division of the normalized angle frequency is 1000.
- **Channel II**
  The group delay difference in the pass band edge and the central frequency is less than 10 symbol gaps with trivial jitter. Other parameters are the same to those of the channel I.

Figs. 4(a) and 4(b) give the wave form of the impulse response of the group delay channel I and II, respectively. Figs. 5 and 6 present the curves of the amplitude-to-frequency and group delay character, respectively. The curves of the amplitude-to-frequency of channel I is stable and the suppression of the side lobe is close to 30 dB. In this channel, the group delay difference in the pass band edge and the central frequency is just 5 symbol gaps with trivial jitter.

$$\hat{\nabla}_{Bk} = 2C \cdot \begin{pmatrix} \alpha_{1,1}^{(k)} \cdot (R_2 - 2\left|y_1^{(k)}\right|^2) & \cdots & \alpha_{L,1}^{(k)} \cdot (R_2 - 2\left|y_L^{(k)}\right|^2) \\ \vdots & \ddots & \vdots \\ \alpha_{1,L}^{(k)} \cdot (R_2 - 2\left|y_1^{(k)}\right|^2) & \cdots & \alpha_{L,L}^{(k)} \cdot (R_2 - 2\left|y_L^{(k)}\right|^2) \end{pmatrix} \cdot \begin{pmatrix} y_1^{(k)}(R_2 - \left|y_1^{(k)}\right|^2) \\ y_2^{(k)}(R_2 - \left|y_2^{(k)}\right|^2) \\ \vdots \\ y_L^{(k)}(R_2 - \left|y_L^{(k)}\right|^2) \end{pmatrix}. \tag{36}$$

TABLE 1. Flow chart of the entire blind adaptive IBCMA-DD equalization.

Procedures of the parallel blind adaptive IBCMA-DD equalization.

(1) Initialization

(1.1) The tap coefficient vector of the equalizer, *i.e.*, $W_k = [w_1, w_2, \cdots, w_L]^T$, is assigned with initial value as $W_1 = [1, 0, \cdots, 0]^T$.

(1.2) μ_{IBCMA} is calculated and configured by numerical simulations of several pre-experiment of the same data set from the received signals.

(1.3)The constant modulus parameter R_2 is calculated as $R_2 = \frac{E(|a_n|^4)}{E(|a_n|^2)}$.

(2) IBCMA for the raw equalization in the capturing stage

(2.1) The received signals put into the equalizer is firstly parallel organized in the form of $\chi_k = [X_{(k-1)L+1}, \cdots, X_{kL}]^T = \begin{pmatrix} x_{(k-1)L+1} & \cdots & x_{kL} \\ \vdots & \ddots & \vdots \\ x_{kL} & \cdots & x_{(k+1)L-1} \end{pmatrix}$.

(2.2) The temporal output of the equalizer is calculated as $Y_k = \chi_k \cdot W_k^*$.

(2.3) The error vector is composed of L error variables as the elements and it is generated as $\varepsilon_k = \begin{pmatrix} e_1^{(k)} \\ e_2^{(k)} \\ \vdots \\ e_L^{(k)} \end{pmatrix} = \begin{pmatrix} y_1^{(k)}(R_2 - \left|y_1^{(k)}\right|^2) \\ y_2^{(k)}(R_2 - \left|y_2^{(k)}\right|^2) \\ \vdots \\ y_L^{(k)}(R_2 - \left|y_L^{(k)}\right|^2) \end{pmatrix}$.

(2.4) The gradient vector for the update of the tap coefficient vector is computed as $\tilde{\nabla}_{Bk} = \begin{pmatrix} \sum_{i=1}^{L} \alpha_{i,1}^{(k)} \cdot (R_2 - 2 \cdot \left|y_i^{(k)}\right|^2) \cdot (e_i^{(k)})^* \\ \sum_{i=1}^{L} \alpha_{i,2}^{(k)} \cdot (R_2 - 2 \cdot \left|y_i^{(k)}\right|^2) \cdot (e_i^{(k)})^* \\ \vdots \\ \sum_{i=1}^{L} \alpha_{i,L}^{(k)} \cdot (R_2 - 2 \cdot \left|y_i^{(k)}\right|^2) \cdot (e_i^{(k)})^* \end{pmatrix}$. Besides, to simplify the computation, $\hat{\nabla}_{Bk}$ is replaced by $\tilde{\nabla}_{Bk}$ without the additional constant coefficient C, which can be incorporated into the step size parameter μ_{IBCMA} in numerical simulations.

(2.5) The tap coefficient vector of the equalizer is updated iteratively and it is calculated as $W_{k+1} = W_k - \mu_{IBCMA} \cdot \tilde{\nabla}_{Bk}$.

(2.6) Calculate the 2-norm of $\tilde{\nabla}_{Bk}$ as $\left\|\tilde{\nabla}_{Bk}\right\|_2$. If it is larger than the switch threshold Γ, goto Step (2.2) for much more equalization iteration. Otherwise, go to the Step (3) for the successive tracking stage of equalization. The switch threshold is mainly generated numerically in simulation experiment, where the mean square errors (MSEs) decrease to some extent to open the eye in the eye pattern of the modulated signals.

(3) DD mode for the fine equalization in the tracking stage

The DD mode is performed in the same way of the block LMS equalization in [18] and the difference is the expected response of received signals. The hard decision of the pre-equalized signals by the IBCMA is employed as the expected response just as the training sequence in the above block LMS algorithm. Finally, the much finer equalization is accomplished by the block LMS algorithm and the result is just the final outcome of the entire IBCMA-DD.

For the channel II, there is similar results, except that the suppression of the side lobe is close to 26 dB. the group delay difference in the pass band edge and the central frequency is less than 10 symbol gaps with a little larger jitter than that of channel I. Here, we mainly focus on the IBCMA-DD equalization itself, rather than the entire channel model of the TWTA with the effect of PA (memoryless, AM/AM, AM/PM, memory effect). So, a typical nonlinear group delay model

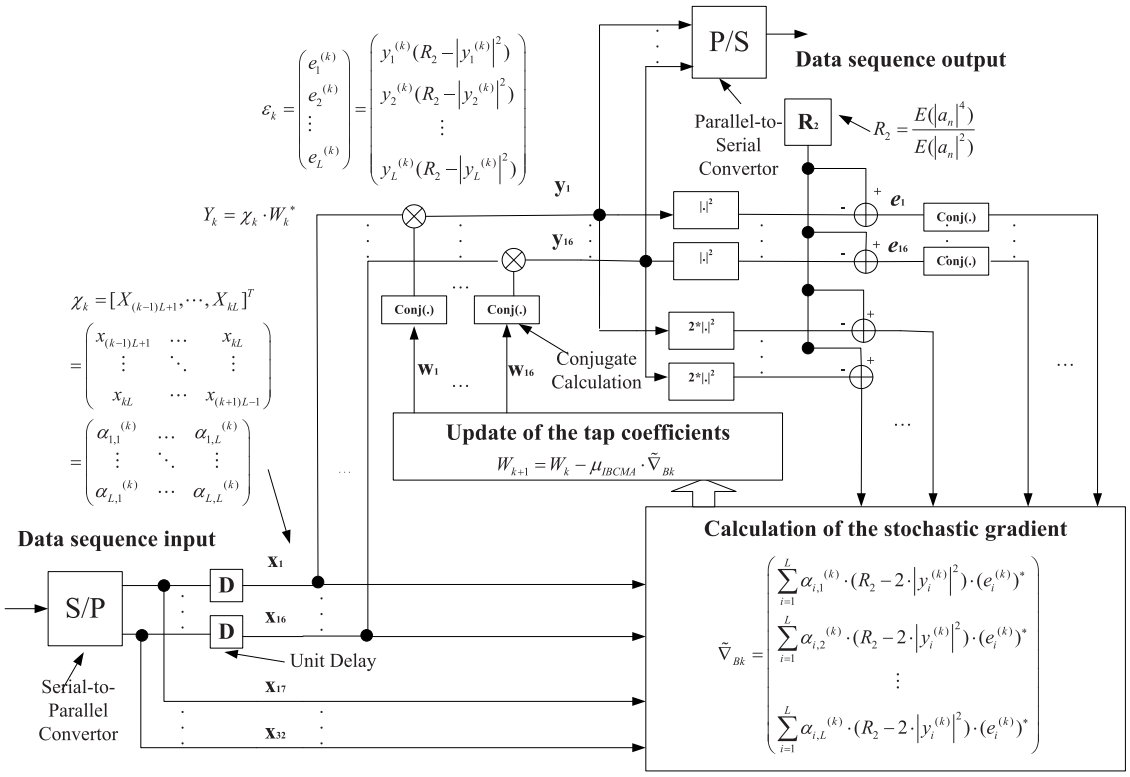

FIGURE 2. Block diagram of the blind adaptive IBCMA equalization scheme (*L*=16).

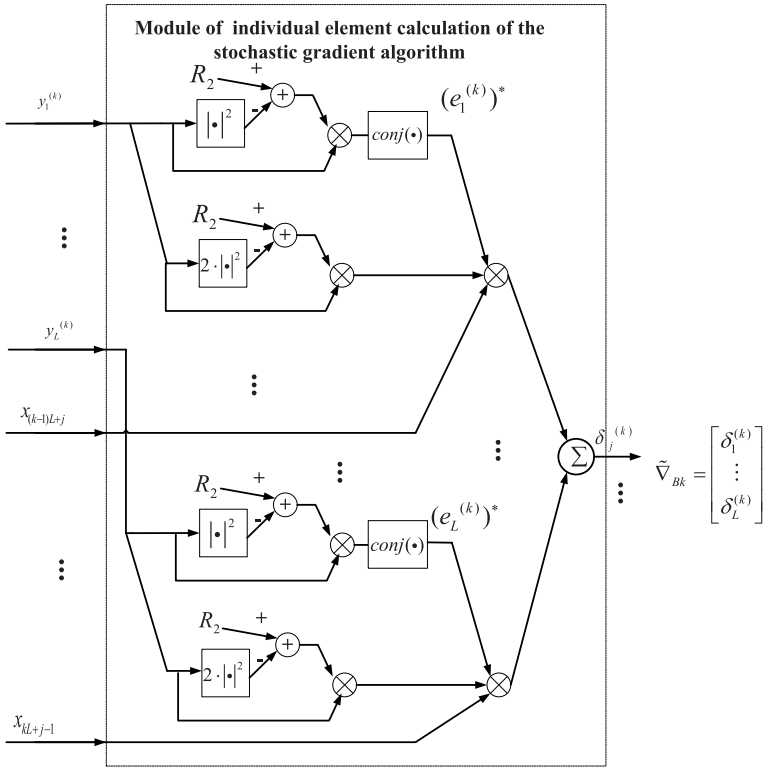

FIGURE 3. Block diagram of the stochastic gradient calculation module.

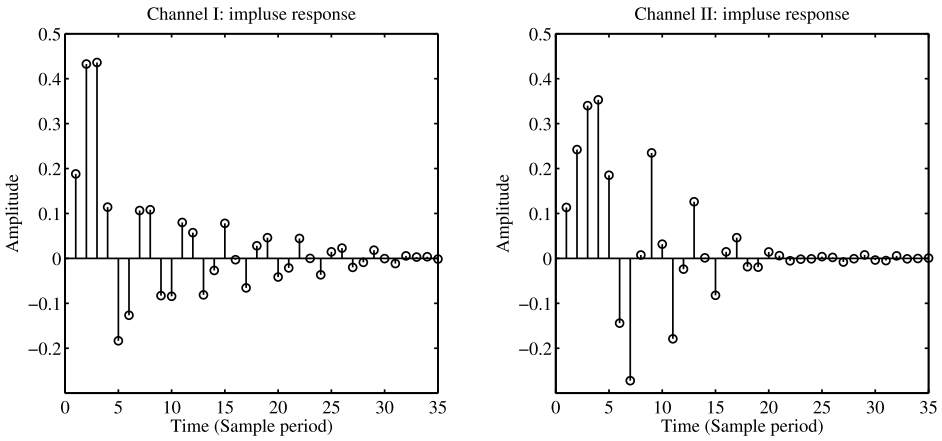

FIGURE 4. Channel impulse response for the group delay effect. (a) Impulse response of Channel I. (b) Impulse response of Channel II.

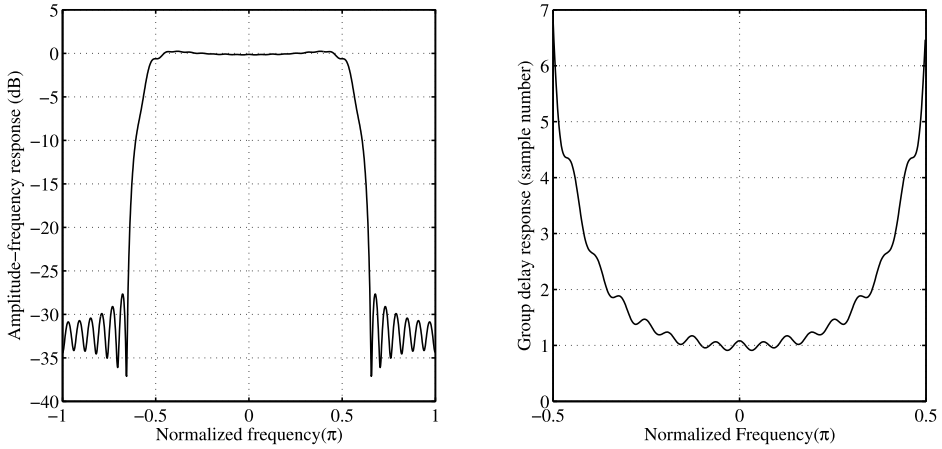

FIGURE 5. Curves of the amplitude-to-frequency and group delay character of channel I.

is just cited for the specific satellite transmission model in 29 and they are clearly illustrated in subsection IV-A as Channels I and II. The effect of PA is actually merged into the TWTA channel model for the simulations in successive equalization.

B. NUMERICAL SIMULATIONS AND ANALYSES OF THE PARALLEL BLIND ADAPTIVE IBCMA-DD EQUALIZATION

The parameters for the simulation of the proposed IBCMA based parallel blind adaptive equalization are listed as follows. The implementation of the proposed IBCMA is considered in the form of $T/4$ fractionally spaced blind equalization to improve the effect of convergence. The quadrate phase shift keying (QPSK) modulation is adopted in transmissions. The total length of the bit sequence is 3.2×10^5. The transmission channel is characterized with the group delay and the noises at the SNRs range from -2 to 10 dB. The taps of the equalizer with the IBCMA and BLMS DD mode is 16, with the tap step of them as 0.0025 and 0.0008, respectively. Channel condition is considered as severe nonlinear group delay channel of I and II with the AWGNs mentioned above. The coefficient vector of the impulse response of the group delay channel is chosen according to the tap coefficients from two channels of I and II shown in Fig. 4, respectively. The length of a data frame is 4000 bits with 80 independent rounds to generate a total bit frame of 3.2×10^5 in simulations. The switch threshold between the IBCMA and DD mode is 0.0642 and it is actually the value of the block mean square error for excellent work of the DD mode acquired by numerical simulations. With the above simulation parameters, the proposed two-stage IBCMA-DD is simulated for the BER performance. The tap length of the equalizer and also the block size as L in (19) are all selected as 16. The initial value of tap-weight vector is the L-dimension vector $[1, 0, \cdots, 0]^T$. The step-size parameter, μ_{IBCMA}, in the equalization, is a small value and need to be properly selected by numerical simulations to guarantee the convergence.

In simulations, we mainly simulate and analyze both the MSE characters and BER performance of the proposed schemes with their counterparts for comparison, respectively. They are presented as follows.

1) SIMULATIONS AND ANALYSES OF THE MSE CHARACTERS

The convergence effect of the equalization is shown in the scatter plot of Fig. 7 and it is mainly assessed by the MSE.

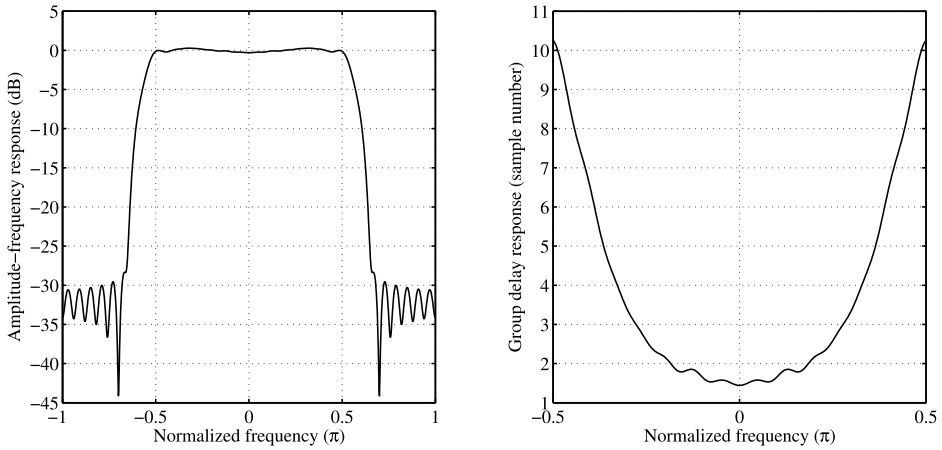

FIGURE 6. Curves of the amplitude-to-frequency and group delay character of channel II.

In Fig. 7, the group delay channel polluted QPSK signals are rectified after the proposed IBCMA and the scattered signals are convergent to the 4 constellation points in the scatter plot. Then, the raw verification of the proposed scheme can be made to equalize and combat the ISI caused by the above two satellite group delay channels. By (23), the estimation of the block mean square error (BMSE) can be expressed as $\underset{k}{\hat{BMSE}} = \sum_{i=1}^{L} \left| e_i^{(k)} \right|^2$ to evaluate the effect according to the criterion of the block MMSE. By computer simulations, the curves of the estimated Block MSE for the proposed IBCMA are shown in Figs. 8 and 9 with respect to the two specific group delay channels of I and II, respectively.

In Figs. 8 and 9, the trend of gradually reduced MSE with equalization iterations although there is still some dithering in the curves. The dithering effect of the scheme is mainly caused by the character of the group delay channel and the stochastic gradient estimation is different with the actual gradient estimation. From the MSE curves of both the IBCMA and CMA in the above two MSE experiments, the IBCMA acquires a much faster convergence than that of the CMA. However, after the convergence, *i.e.*, the stable fluctuate status of the MSE curves, the CMA obtains a little better MSE performance than that of the IBCMA. This phenomenon can be explained as follows. The CMA adopts the criterion of the MMSE for the adaptive equalization update, while the IBCMA employs the block MMSE. The former is more accurate in the estimation and update of every individual tap coefficient of the equalization filter. Thus the IBCMA loses some accuracy of the final equalization performance, but it obtains fast equalization at the cost of some more computational complexity. Finally, the BER is obtained from the simulation as 0.016429 for equalization validation and the entire scheme can be concluded as convergence, since the performance is improved different from the scheme of no equalization.

2) SIMULATIONS AND ANALYSES OF THE BER PERFORMANCE

Generally, the convergence effect of the equalization can also be indirectly evaluated by the BER SNR curves. We simulate the QPSK modulation system of 3.2×10^5 samples with the IBCMA-based FSE by the method of Monte Carlo simulation for independent 80 times. The BER is not calculated until the equalizer is convergence. Finally, the simulation results of the BER performance are shown in Fig. 9 and Fig. 10 with respect to the above two channels of I and II, respectively. The proposed IBCMA-DD scheme obtains rather good characters of convergence under such group delay channels especially at high SNRs. Because the residual distortion is caused by the stochastic gradient in place of the expected gradient and step-size parameter has not properly selected at low SNR, the curves of our scheme has still some disparity when compared with the theoretical BER SNR curve of the QPSK. But it shows good convergence and can be simply implemented as practical parallel blind equalization under severe group delay channel distortions.

Initially, we simulate and verify the proposed IBCMA-DDM scheme at a severe Proakis ISI channel III with the group delay response function in the linear case. The discrete-time channel characteristics, *i.e.*, the coefficient vector of impulse response of such ISI channel, is then chosen and expressed as $[0.2270.460.6880.4600.227]^T$ with constant group delay of 2 samples (in [26], P.654, Fig. 9.4-5(c)). It is actually a non-minimum phase system and cannot be perfectly equalized by traditional adaptive equalization of finite length of taps. In Fig. 10, the performance of the IBCMA is still a little poorer than that of the CMA by about 2dB at BER of 10^{-2}, but it achieves fast equalization by the parallel structure. The IBCMA has a little more performance loss than CMA, because the criterion of error correcting in the former is by the block MMSE, while that in the latter is just by the MMSE. The MMSE is surely more accurate for the estimation of every unique sample due to the nature of larger residual estimation distortion in the block MMSE.

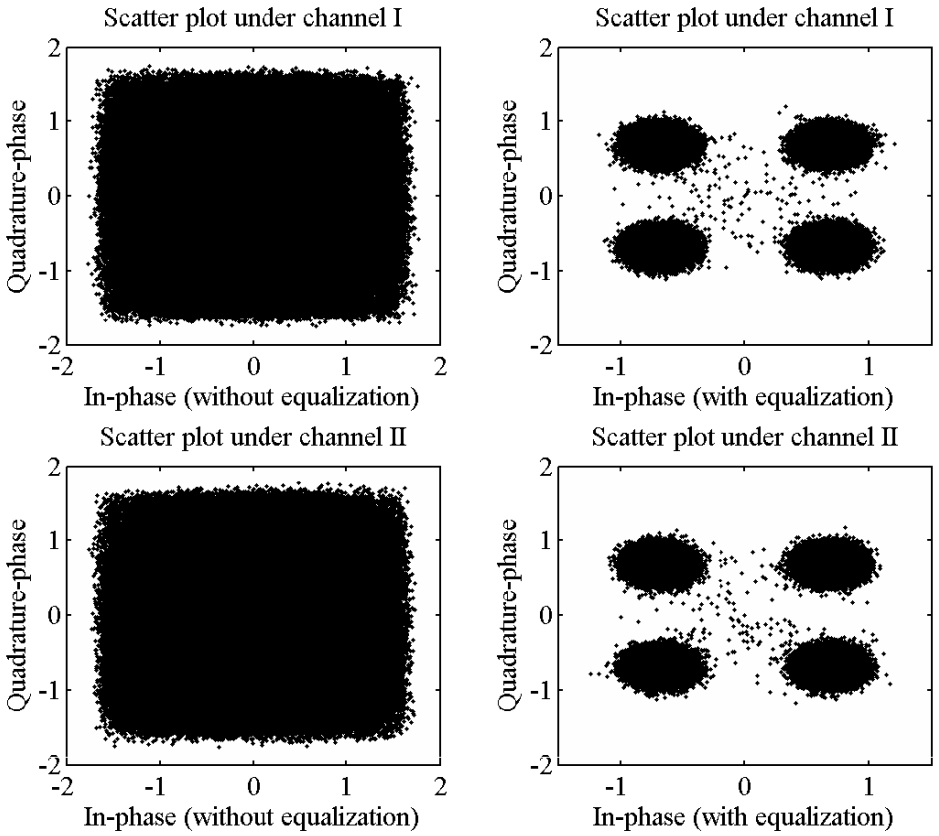

FIGURE 7. Scatter plots by the IBCMA equalization under channel I and II (3.2×10^5 samples).

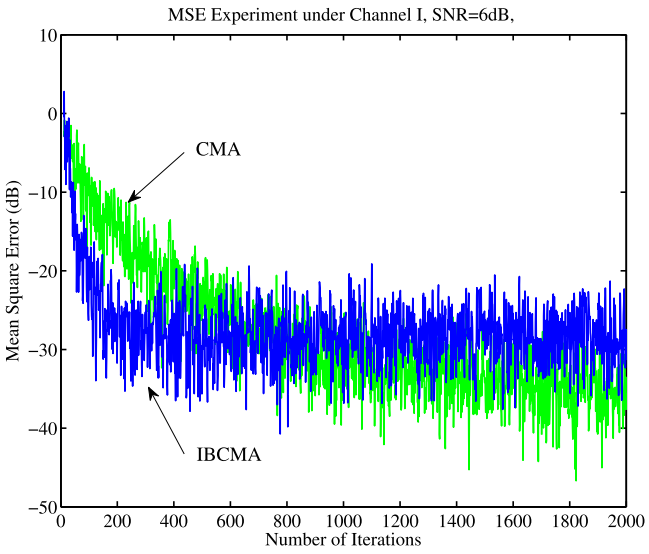

FIGURE 8. MSE of the IBCMA (Channel I, SNR=6) with the counterparts of the CMA.

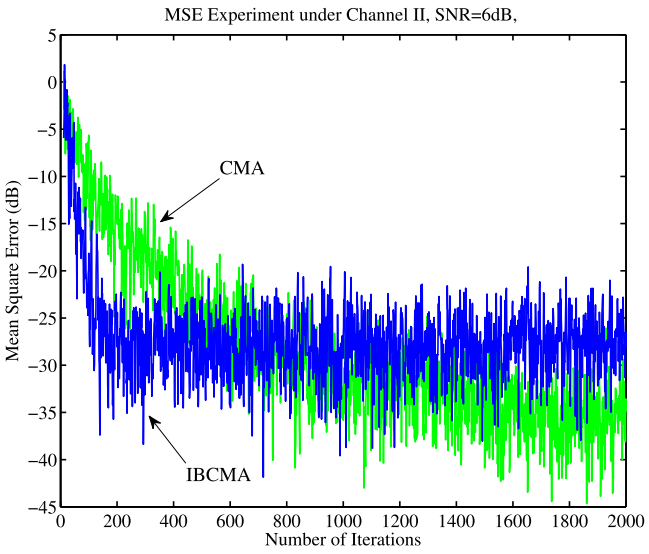

FIGURE 9. MSE of the IBCMA (Channel II, SNR=6) with the counterparts of the CMA.

However, they all decrease slowly at high SNRs due to the fact that they are all blind equalization and the expected reference signals in the adaptive update in iterative equalization is not exact the actual value for the required comparison. However, the DD mode can be the perfect compensation of the blind equalization since the expected reference signals are hard decision of the equalized ones at high SNRs and they are almost the true reference value for the required ones. And the simulation results for the IBCMA-DD scheme also validate the good performance, where the performance approaches the ideal one. It represents good convergence and the performance loss is within 0.3 dB at BER of 10^{-5}.

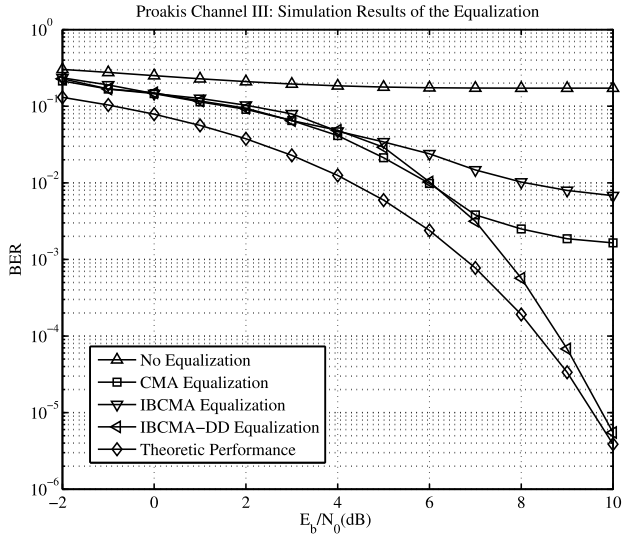

FIGURE 10. BER performance of the proposed IBCMA-DD scheme at severe Proakis channel III with group delay response function in the linear case.

It can be explained as follows. Due to the residual distortion from the stochastic gradient in place of expected gradient and the improperly selected step-size parameter at each bit SNR, the curve of the proposed scheme still has some disparity when compared with the theoretic BER curve of the QPSK. However, with the help of error correcting channel codes, the whole communication system achieves significant BER performance for practical applications. In addition, the problems about the phase rotation correction, large residual errors and slow convergence and so on have been totally discussed and solved perfectly in section I, which eliminates all deficiencies of the proposed IBCMA-DD scheme in practice. Therefore, the proposed scheme can be simply implemented as practically parallel blind equalizer to obtain faster speed of equalization than that in the serial equalizer of digital modems under severe channel distortions.

Subsequently, in Figs. 11 and 12, the proposed IBCMA-DD scheme obtains good BER performance and they closely approach the ideal theoretic QPSK performance curves. The performance of the proposed IBCMA scheme is a little poorer than that of the CMA. Different channels have little influence on the equalization and the BER curves of them are similar under the two channels, where Channel II has five more symbol period than that of Channel I. However, the curves of the individual CMA and IBCMA cannot approach the theoretic curve at high SNRs (*e.g.*, SNR>8dB). In addition, under such high SNR circumstance, they almost improved less with the increase of the SNRs. With the aid of the DD mode, the performance of the proposed scheme can approach the ideal performance. These phenomena can be explained as follows. First, the CMA and the IBCMA are blind equalization and they used the high order statistics to finish the adaptive equalization. Hence, the expected response for the specific symbol is exactly the average reference value and it is not accurately consistent to it. Therefore, the equalization performance of the proposed IBCMA scheme is poorer than that of the classic LMS algorithm, which possesses the good property of approaching ideal performance. But it needn't occupy additional bandwidth to transmit true counterpart training data for comparison and equalization iteration, thus it is more suited for use in multipoint network transmission. Since the DD possesses good equalization performance with opened eye pattern of modulated signals especially in high SNRs, it can be a perfect amendment for the proposed IBCMA to achieve good performance very close to the ideal demodulation. The proposed parallel IBCMA-DD employs the block MMSE criterion to achieve the convergence and it brings much more residual errors other than that of the serial CMA. So the performance is still a little poorer in the IBCMA. Although the performance of the proposed IBCMA is a little poorer than that of the classical CMA, it has indeed speeded up the equalization and it reaches the threshold for the effective DD equalization, which performs excellent at high SNRs. Therefore, aided by the DD mode, the proposed IBCMA perform quite well, and the joint IBCMA-DD scheme achieves perfect results close to the ideal performance. Then, the simulation results are presented in an adequate manner with comparison of the original CMA and also the ideal demodulation curve and the proposed joint IBCMA-DD scheme is superior to the classic blind CMA equalization algorithms too. Second, we use a length-16 taps equalizer filter to overcome the nonlinear group delay of Channel I and II with 5 and 10 symbol period of the filter group delay. From simulation results in Figs. 11 and 12, they exhibit excellent equalization performance and the enough length of the equalizer taps can totally compensate the channel distortion adaptively. The nature of it lies in the fact that the impulse response of the equalizer can be constructed as the perfect deconvolution of that of the channel distortion. Subsequently, the proposed scheme with such tap length can cover the main distortion in the form of the adaptive blind equalization. Finally, at high SNRs, the BER curves of both the IBCMA and CMA become flat, because the residual interference of the blind equalization rather than the noises preside the equalization on such circumstance. As blind CMA-like equalization by statistical expected parameters in equalization computation rather than the true training sequence ones, it is inevitable to unable achieve ideal performance and the residual interference after the blind equalization predominate the final performance.

In summary, the proposed IBCMA-DD obtains rather good convergence under such sever nonlinear group delay channels especially at high bit signal-to-noise ratio (bit SNR or E_b/N_0). Because the residual distortion is caused by the stochastic gradient in place of expected gradient and the step-size parameter has not properly selected for conditions at each bit SNR, the curve of our scheme has still some disparity when compared with the theoretic BER curve of the QPSK. The IBCMA has still a little more performance loss than that of the CMA because the criterion of error correcting in the former is

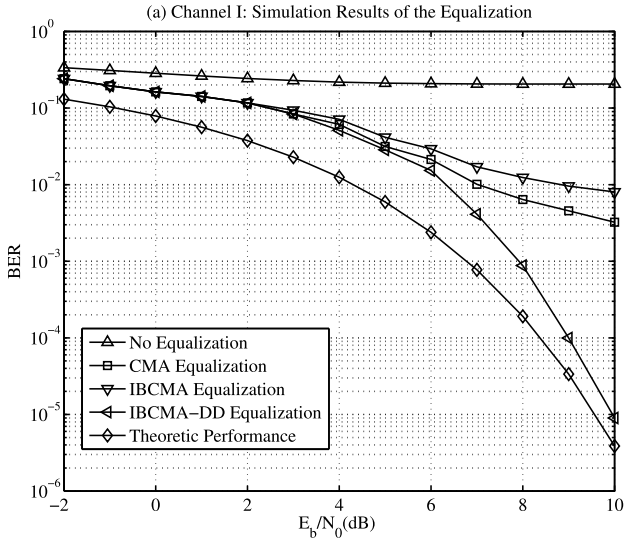

FIGURE 11. BER performance of the proposed IBCMA-DD scheme at satellite group delay channel I in the nonlinear case.

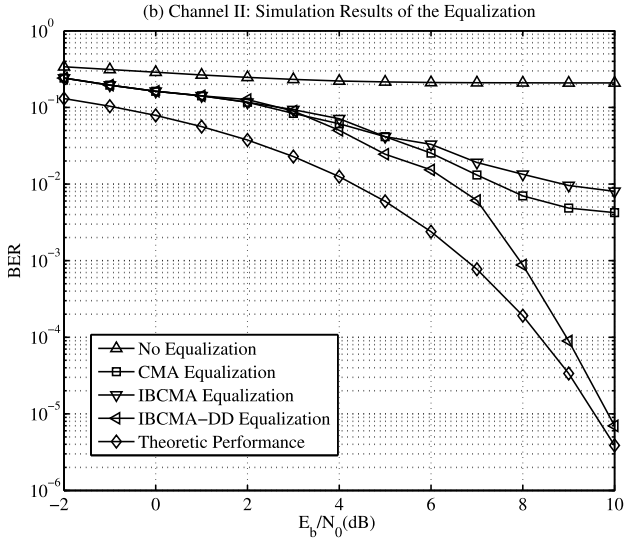

FIGURE 12. BER performance of the proposed IBCMA-DD scheme at satellite group delay channel II in the nonlinear case.

by the block MMSE, while that of the latter is by the MMSE, which is more accurate in the estimation of every individual sample. Although the performance of the suggested IBCMA shows some difference compared with the theoretic curves and even shows a little worse performance than the CMA, by the aid of DD mode, it represents good convergence and the error rate is still within 3 dB of the error rate achieved at low E_b/N_0 (<7dB). However, by commonly used error correct codes, the entire system can achieve satisfied BER performance in practice. Therefore, the proposed IBCMA-DD scheme can be implemented as practically parallel blind equalizer to obtain the faster convergence speed than that of the serial CMA equalizer in digital modems under severe nonlinear group delay distortion.

V. CONCLUSION

In this paper, a new parallel blind adaptive equalization of improved block constant modulus algorithm and decision-directed mode, *i.e.*, IBCMA-DD, is proposed for the implementation of broadband digital satellite modems with high data rate. The IBCMA and DD mode are combined together to overcome the non-linear group delay ISI efficiently. The signal sequences can be equalized by L samples at a time for fast and accurate equalization. The main contributions are concluded as follows. First, nonlinear group delay models are modeled and constructed for satellite channels. Second, the block MMSE-based performance criterion is derived for the IBCMA with a gradient estimate of a correction between the desired and input signals. Third, practical IBCMA-DD scheme is proposed to accelerate the parallel blind equalization, and thus it both improves the spectrum efficiency and compensates the residual mean square excess errors and phase rotation. Simulations show that it possesses good robustness and stability with respect to severe channel distortion. In conclusion, the proposed equalization obtains efficient parallel blind equalization at the cost of a little performance loss, which endows it a good application in nonlinear group delay equalization in terrestrial-space satellite communications.

REFERENCES

[1] H. Li, Z.-G. Wang, and H.-J. Wang, "Research on high speed parallel blind equalization algorithm," in *Proc. Int. Conf. Comput. Netw. Commun. Technol. (CNCT)*. Amsterdam, The Netherlands: Atlantis Press, 2017, pp. 1–5.

[2] G. Malik and A. Singh, "Adaptive equalization algorithms: An overview," *Int. J. Adv. Comput. Sci. Appl.*, vol. 2, no. 3, pp. 62–67, 2011.

[3] J. Treichler and B. Agee, "A new approach to multipath correction of constant modulus signals," *IEEE Trans. Acoust., Speech, Signal Process.*, vol. ASSP-31, no. 2, pp. 459–472, Apr. 1983.

[4] R. Johnson, P. Schniter, T. J. Endres, J. D. Behm, D. R. Brown, and R. A. Casas, "Blind equalization using the constant modulus criterion: A review," *Proc. IEEE*, vol. 86, no. 10, pp. 1927–1950, Oct. 1998.

[5] Y. Sato, "A method of self-recovering equalization for multilevel amplitude-modulation systems," *IEEE Trans. Commun.*, vol. C-23, no. 6, pp. 679–682, Jun. 1975.

[6] D. Godard, "Self-recovering equalization and carrier tracking in two-dimensional data communication systems," *IEEE Trans. Commun.*, vol. C-28, no. 11, pp. 1867–1875, Nov. 1980.

[7] M. T. M. Silva and M. D. Miranda, "Tracking issues of some blind equalization algorithms," *IEEE Signal Process. Lett.*, vol. 11, no. 9, pp. 760–763, Sep. 2004.

[8] R. Wang, Y. Wang, and X. Hu, "Simulation and analysis of influence of group delay distortion on satellite-to-ground and satellite-to-satellite link channel," in *Signal and Information Processing, Networking and Computers*, vol. 917. Singapore: Springer, Jul. 2022, pp. 607–615.

[9] A. L. Swindlehurst, "Normalized adaptive decision directed equalization," *IEEE Signal Process. Lett.*, vol. 5, no. 1, pp. 18–20, Jan. 1998.

[10] V. Weerackody, S. A. Kassam, and K. R. Laker, "Convergence analysis of an algorithm for blind equalization," *IEEE Trans. Commun.*, vol. 39, no. 6, pp. 856–865, Jun. 1991.

[11] W. Chung and J. P. LeBlanc, "The local minima of fractionally-spaced CMA blind equalizer cost function in the presence of channel noise," in *Proc. IEEE Int. Conf. Acoust., Speech Signal Process.*, Boston, MA, USA, May 1998, pp. 1–9.

[12] J. R. Treichler, V. Wolff, and C. R. Johnson, "Observed misconvergence in the constant modulus adaptive algorithm," in *Proc. 24th Asilomar Conf. Signals, Syst. Comput.*, Pacific Grove, CA, USA, 1985, pp. 21731–21744.

[13] G. Scarano, A. Petroni, M. Biagi, and R. Cusani, "Blind fractionally spaced channel equalization for shallow water PPM digital communications links," *Sensors*, vol. 19, no. 21, p. 4604, Oct. 2019.
[14] Y. Li and Z. Ding, "Global convergence of fractionally spaced Godard (CMA) adaptive equalizers," *IEEE Trans. Signal Process.*, vol. 44, no. 4, pp. 818–826, Apr. 1996.
[15] I. Fijalkow, A. Touzni, and R. Treichler, "Fractionally spaced equalization using CMA robustness to channel noise and lack of disparity," *IEEE Trans. Signal Process.*, vol. 45, no. 1, pp. 56–66, Jan. 1997.
[16] J. Treichler and M. Larimore, "New processing techniques based on the constant modulus adaptive algorithm," *IEEE Trans. Acoust., Speech, Signal Process.*, vol. ASSP-33, no. 2, pp. 420–431, Apr. 1985.
[17] W. Hu, Z. Wang, R. Mei, and M. Lin, "A simple and robust equalization algorithm for variable modulation systems," *Electronics*, vol. 10, no. 20, p. 2496, Oct. 2021.
[18] G. Clark, S. Mitra, and S. Parker, "Block implementation of adaptive digital filters," *IEEE Trans. Acoust., Speech, Signal Process.*, vol. ASSP-29, no. 3, pp. 744–752, Jun. 1981.
[19] B. Q. Vuong, R. Gautier, H. Q. Ta, L. L. Nguyen, A. Fiche, and M. Marazin, "Joint semi-blind self-interference cancellation and equalisation processes in 5G QC-LDPC-encoded short-packet full-duplex transmissions," *Sensors*, vol. 22, no. 6, p. 2204, Mar. 2022.
[20] S. Guo, J. Wang, H. Ma, and J. Wang, "Modified blind equalization algorithm based on cyclostationarity for contaminated reference signal in airborne PBR," *Sensors*, vol. 20, no. 3, p. 788, Jan. 2020.
[21] Z. Pan, C. Xie, H. Wang, Y. Wei, and D. Guo, "Blind turbo equalization of short CPM bursts for UAV-aided Internet of Things," *Sensors*, vol. 22, no. 17, p. 6508, Aug. 2022.
[22] S. O. Haykin, *Adaptive Filter Theory*. 5th ed. Upper Saddle River, NJ, USA: Prentice-Hall, 2013, pp. 123–135.
[23] I. Fijalkow, C. E. Manlove, and C. R. Johnson, "Adaptive fractionally spaced blind CMA equalization: Excess MSE," *IEEE Trans. Signal Process.*, vol. 46, no. 1, pp. 227–231, Jan. 1998.
[24] O. Shalvi and E. Weinstein, "New criteria for blind deconvolution of nonminimum phase systems (channels)," *IEEE Trans. Inf. Theory*, vol. 36, no. 2, pp. 312–321, Mar. 1990.
[25] J. K. Tugnait, "Comments on 'New criteria for blind deconvolution of nonminimum phase systems (channels)'" *IEEE Trans. Inf. Theory*, vol. 38, no. 1, pp. 210–212, Jan. 1992.
[26] J. G. Proakis, *Digital Communications*, 5th ed. New York, NY, USA: McGraw-Hill, 2008, pp. 389–395.
[27] W. Tranter and K. Shanmugan, *Principles of Communication Systems Simulation With Wireless Applications*. Upper Saddle River, NJ, USA: Prentice-Hall, 2004, pp. 432–456.
[28] H. Gao and X. Li, "Simulation and analysis of influence of group delay distortion on performance of DBF system," in *Proc. Nat. Conf. Inf. Technol. Comput. Sci.* Amsterdam, The Netherlands: Atlantis Press, 2012, pp. 534–537.
[29] J. H. Park, D. H. Shin, B. H. Chung, and S. P. Lee, "Development of experimental Ka-band satellite communications payload for wideband multimedia services," in *Proc. Joint Conf. Satell. Telecommun.*, Tokyo, Japan, vol. 100, Dec. 2000, pp. 65–78.

YING CHEN received the B.S. and M.S. degrees in communication engineering from Hangzhou Dianzi University, Hangzhou, Zhejiang, China, in 2000 and 2006, respectively.

She is currently an Associate Professor with the Information Engineering School, Hangzhou Dianzi University. Her research interests include modern wireless communications and wireless IoT.

GEQI WENG received the B.S. degree in electrical engineering from the Nanjing University of Aeronautics and Astronautics, Nanjing, Jiangsu, China, in 2000, and the M.S. degree in communication and information system from the Zhejiang University of Technology, Hangzhou, Zhejiang, China, in 2004.

He is currently the CTO of Hangzhou Kylin Technology Company Ltd. His research interests include modern wireless communications and coding and performance analysis of wireless networks.

SHENJI LUAN received the B.S. and M.S. degrees in communication engineering from Hangzhou Dianzi University, Hangzhou, Zhejiang, China, in 2002 and 2005, respectively, and the Ph.D. degree in control science and engineering from the Zhejiang University of Technology, Hangzhou, in 2015.

He was a Visiting Scholar with Zhejiang University, Hangzhou, in 2020. He is currently an Associate Professor with the Information Engineering School, Hangzhou Dianzi University. His research interests include modern wireless communications and coding and performance analysis of wireless networks.

YANHAI SHANG received the Ph.D. degree in signal processing from the Beijing Institute of Technology, Beijing, China, in 2004.

He was a Postdoctoral Researcher of radar imaging with the University of Electronic Science and Technology of China, Chengdu, Sichuan, China, from 2005 to 2007. He is currently with the Information Engineering School, Hangzhou Dianzi University, Hangzhou, China. His research interests include communication and information theory and statistical signal processing.

CHAO LIU received the B.S. and Ph.D. degrees in information and communication engineering from the School of Electronic Information and Communications, Huazhong University of Science Technology, Wuhan, China, in 2000 and 2005, respectively.

He is currently an Associate Professor with the School of Communication Engineering, Hangzhou Dianzi University, Hangzhou, China. His research interests include modern wireless communication and coding and MIMO multi-user detection.

JIANRONG BAO (Senior Member, IEEE) received the B.S. degree in polymeric materials and engineering and the M.S. degree in communication and information system from the Zhejiang University of Technology, Hangzhou, China, in 2000 and 2004, respectively, and the Ph.D. degree in information and communication engineering from the Department of Electronic Engineering, Tsinghua University, Beijing, China, in 2009.

He was a Postdoctoral Researcher with Zhejiang University, from 2011 to 2013, and Southeast University, from 2014 to 2017. He was a Visiting Scholar with Columbia University, New York, NY, USA, in 2015. He is currently a Professor with the School of Communication Engineering, Hangzhou Dianzi University, Hangzhou. His research interests include modern wireless communications, cognitive radio, information theory and coding, communication signal processing, and wireless sensor networks. He received several provincial awards for technological invention, including the Zhejiang Provincial Awards for Technological Invention of the Third Grade.